Leakage flux analysis in toroidal core with circular cross section based on analytic calculation

Li Tian, Cai-Xia Tao, Ming-Xing Tian

School of Automation and Electrical engineering Lanzhou Jiao Tong University

88 West Anning Rd. Lanzhou Gansu China

Tianli @mail.lzjtu.cn http://mail.lzjtu.edu.cn/

Abstract: It is important to understand the leakage flux distributions of toroidal core under the condition of the coil is wound partially on the surface of the core, and the magnetic permeability is not very large. In this paper, formulas of the electrical field intensity and magnetic field intensity in toroidal core with circular cross section are derived, as the leakage fluxes to be considered. The formula of eddy-current power losses are also derived based on the electrical field intensity formula. The calculated results of the eddy-current power losses are in good agreement with the formula which is derived from the self impedance of coil. Effects of frequency, magnetic permeability and distribution of windings on leakage fluxes are analyzed. The results show the formulas accurately predicted the case when magnetic permeability of the core is very large or the coil is wound densely and uniformly on the surface of the core, the leakage fluxes are very small and can be neglected. Magnetic fluxes decreases with frequency increasing , while the proportion of leakage fluxes increase with frequency increasing. It has been shown that leakage fluxes limit the upper frequency of operation.

Keywords: toroidal core；electromagnetic field distributions; leakage fluxes；eddy-current power losses

1 Introduction

The toroidal core has been widely used in electronic circuits [1-2]. Power losses and leakage fluxes in the core become more pronounced with energised frequency increasing. Therefore the knowledge of power losses and leakage fluxes at high frequencies becomes more and more important in the design of magnetic components, such as transformers and inductors. Electromagnetic field distribution and power losses in toroidal core have attracted considerable attentions [3-8]. Ying Baiqing investigated magnetic field distributions and eddy-current power losses in toroidal core with an arbitrary cross section by using FEM (finite element method) [4]. K V Namjoshi et al performed researches on magnetic field distributions and eddy-current power losses in toroidal core with rectangular cross section, and then they gave analytical solutions [5-6]. Electromagnetic distributions and iron loss in toroidal core with circular cross section were also studied by Saotome H et al, and the analytical solutions were given [7-8]. Whereas all the previous studies have been mainly focused on the case of magnetic

permeability of the core is very large （ when $\delta = 100 \mathrm{S} \cdot \mathrm{m}^{-1}$, $f = 1\mathrm{MHz}$, $\mu_r > 10^5$ ） or the coil is wound densely and uniformly on the surface of the core, neglecting the leakage fluxes.

(a) Coil on toroidal core

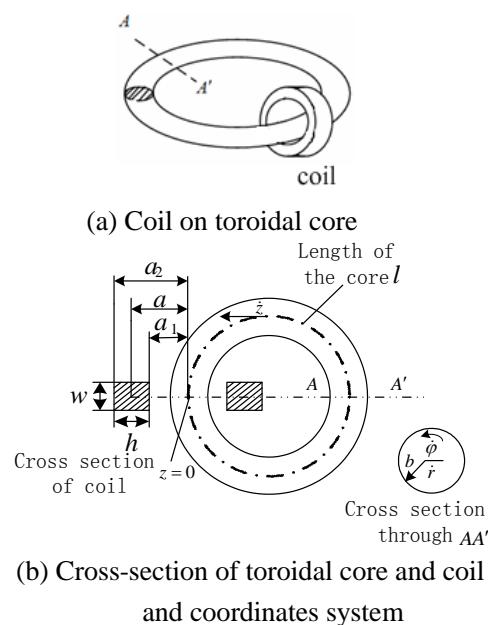(b) Cross-section of toroidal core and coil and coordinates system

Fig.1 Toroidal core under study

In this paper, the diagram of the toroidal core

under study is shown in Fig.1, where coil is wound partially on the surface of the core and magnetic permeability of the core is not very large (when $\delta = 100 \mathrm{S \cdot m^{-1}}$, $f = 1\mathrm{MHz}$, $\mu_r < 10^5$). In this case, leakage fluxes can't be neglected. Therefore, the aim of this study is to present an analytical method for the electrical field and magnetic field distributions in toroidal core with circular cross section, as the leakage fluxes to be considered. Based on the formula of electrical field intensity, a closed-form expression is also derived for the eddy-current power losses.

2 Deduction of formula for the calculation of electrical field in toroidal core

2.1 A filamentary turn on an infinite core

The physical arrangement under study is shown in Fig.2. The core, taken to be infinitely long, is treated as a homogeneous isotropic linear medium of conductivity σ and magnetic permeability μ_2. The core radius is b. A filamentary turn of radius a encircles the core at $z = 0$, and carries a sinusoidal current i_φ, i.e. $i_\varphi = I_\varphi e^{j\omega t}$, where ω is the angular frequency.

Cylinder coordinates r, φ, z are utilized here. The following identities apply on the ground of symmetry:

$$E_r = 0, \qquad E_z = 0, \qquad \partial E_\varphi / \partial \varphi = 0$$

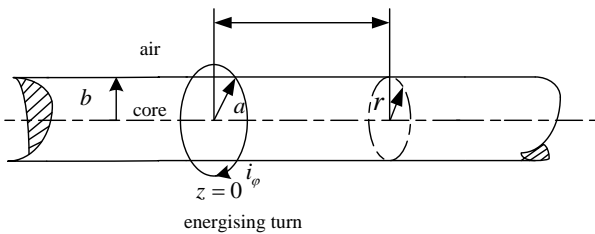$$H_\varphi = 0, \qquad \partial H_r / \partial \varphi = 0, \qquad \partial H_z / \partial \varphi = 0$$

Fig.2 Filamentary turn on infinite cores

Formula of electrical field intensity in the core is derived in Ref. [9], where it is shown as

$$E_{\varphi 1}^* = -\mathrm{j}\omega\mu_1 I_\varphi \frac{I_1(\Gamma r)}{I_1(\Gamma b)} a\beta K_1(\beta a)$$

$$\times \frac{I_1(\Gamma b)\{I_0(\beta b)K_1(\beta b)+I_1(\beta b)K_0(\beta b)\}}{\dfrac{\mu_1}{\mu_2}\Gamma I_0(\Gamma b)K_1(\beta b)+\beta K_0(\beta b)I_1(\Gamma b)} \qquad (1)$$

where

I_0, K_0, I_1, K_1 — the modified Bessel functions.

$\Gamma = \sqrt{\beta^2 + m^2}$

$m^2 = \mathrm{j}\omega\mu_2\sigma$

μ_1 — magnetic permeability of medium outside the core ($\mu_1 \approx \mu_0 = 4\pi\times10^{-7}$).

$E_{\varphi 1}^*$ indicate Fourier integral transform function of $E_{\varphi 1}$

β — the transform parameter.

Solution of $E_{\varphi 1}$ is obtained by Fourier transform inversion.

$$E_{\varphi 1} = -\frac{\mathrm{j}\omega\mu_1 I_\varphi}{2\pi}\int_{-\infty}^{+\infty} aK_1(\beta a)\frac{I_1(\Gamma r)I_1(\beta b)}{I_1(\Gamma b)}$$

$$\times \frac{\beta\dfrac{K_0(\beta b)}{K_1(\beta b)}+\beta\dfrac{I_0(\beta b)}{I_1(\beta b)}}{\beta\dfrac{K_0(\beta b)}{K_1(\beta b)}+\dfrac{\mu_1}{\mu_2}\Gamma\dfrac{I_0(\Gamma b)}{I_1(\Gamma b)}}e^{\mathrm{j}\beta z}\mathrm{d}\beta \qquad (2)$$

with the auxiliary functions defined by:

$$\Phi(\beta) = \frac{g(\beta)+f(\beta)}{g(\beta)+\dfrac{\mu_1}{\mu_2}f(\Gamma)} \qquad (3)$$

$$f(x) = x\frac{I_0(xb)}{I_1(xb)} \qquad (4)$$

$$g(x) = x\frac{K_0(xb)}{K_1(xb)} \qquad (5)$$

Writing the formula of Eqn.2 as

$$E_{\varphi 1} = -\frac{\mathrm{j}\omega\mu_1 I_\varphi}{2\pi}\int_{-\infty}^{+\infty} aK_1(\beta a)$$

$$\times \frac{I_1(\Gamma r)I_1(\beta b)}{I_1(\Gamma b)}\Phi(\beta)e^{\mathrm{j}\beta z}\mathrm{d}\beta \qquad (6)$$

For writing convenience, the formula of Eqn.6 was written as

$$E_{\varphi 1} = \int_{-\infty}^{+\infty} H(a,r,\beta)e^{\mathrm{j}\beta z}\mathrm{d}\beta \qquad (7)$$

2.2 A filamentary turn on toroidal core

In many magnetic components, the core will form a closed magnetic circuit, usually rectangular or toroidal, as shown in Fig.1. The issue of shape is sidestepped by imagining the core to have been cut open and straightened out to its length l (noting that in practice $l/b > 25$ for toroidal core [10], thus neglecting the difference between the inner diameter and outer diameter). A return flux path of zero reluctance is then provide by placing the straightened-out core between two infinite plates of perfect magnetic material ($\mu = \infty$, $\delta = 0$) [9], as shown in Fig.2(a). Let the energizing turn be located

halfway along the straightened core (by choosing to open the actual core at the location most remote from the turn involved), the field is then symmetrical about the plane $z = 0$.
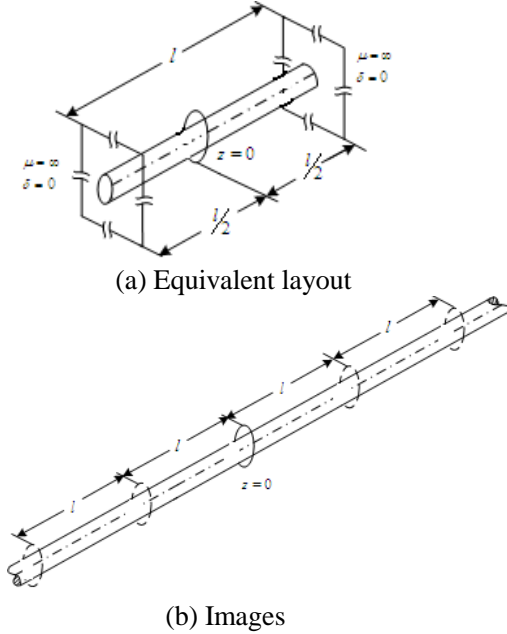

(a) Equivalent layout

(b) Images

Fig.3 Simulation of toroidal core and image turns

Since the plates are infinitely permeable and non-conducting, the lines of flux enter or leave the plates at right angles. Furthermore, a line of flux leaving at the right-hand plate may be legitimately considered to immediately re-enter from the corresponding position on the left-hand plate.

According to mirror image method, the required boundary condition will be equivalently satisfied, relative to $-l/2 \leq z \leq l/2$, if the boundary plates are removed and an infinite number of images introduced along an infinite core in the manner shown in Fig.3(b) (the solid circle indicate actual energizing turn at $z = 0$, the dotted circles indicate image turns). Thus, on the basis of Eqn.7 writing the corresponding electrical field intensity formula for the closed core is simply

$$E_{\varphi 2} = \int_{-\infty}^{+\infty} H(a, r, \beta) \sum_{k=-\infty}^{+\infty} e^{jk\beta l} e^{j\beta z} \mathrm{d}\beta \qquad (8)$$

Noting that

$$\sum_{k=-\infty}^{+\infty} e^{jk\beta l} = \frac{2\pi}{l} \sum_{k=-\infty}^{+\infty} \delta(\beta - \frac{2k\pi}{l})$$

Eqn.8 immediately reduces to

$$E_{\varphi 2} = \frac{2\pi}{l} \sum_{k=-\infty}^{+\infty} H(a, r, \beta_k) e^{j\beta_k z} \qquad (9)$$

where

$$\beta_k = \frac{2k\pi}{l} \qquad (10)$$

On the basis of Eqn.6

$$E_{\varphi 2} = -\frac{j\omega\mu_1 I_\varphi}{l} \sum_{k=-\infty}^{+\infty} aK_1(\beta_k a)$$

$$\times \frac{I_1(\Gamma_k r) I_1(\beta_k b)}{I_1(\Gamma_k b)} \Phi(\beta_k) e^{j\beta_k z} \qquad (11)$$

where

$$\Gamma_k = \sqrt{\beta_k^2 + m^2} \qquad (12)$$

Thus, the closed-core case formally converts the integrals of the infinite-core case to straightforward summations. Noting that single-sided summation is justified, then we have

$$E_{\varphi 2} = E_{\varphi 20} + E_{\varphi 2k} \qquad (13)$$

where

$$E_{\varphi 20} = -\frac{j\omega\mu_1 I_\varphi}{l} \frac{\mu_{2r} I_1(mr)}{m I_0(mb)} \qquad (14)$$

$$E_{\varphi 2k} = -\frac{j\omega\mu_1 I_\varphi}{l} \left[2\sum_{k=1}^{+\infty} aK_1(\beta_k a) \right.$$

$$\left. \times \frac{I_1(\Gamma_k r) I_1(\beta_k b)}{I_1(\Gamma_k b)} \Phi(\beta_k) \cos(\beta_k z) \right] \qquad (15)$$

$\mu_{2r} = \dfrac{\mu_2}{\mu_1}$ —— relative permeability of the core

2.3 A coil on toroidal core

Coil is composed of many turns. We specialize on the usual case of rectangle cross-section of coil as illustrated in Fig.1. The number of turns is N. Then,
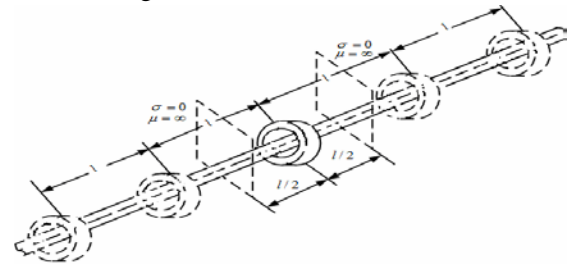
Fig.4 Simulation of toroidal cores and image coils

in a similar manner as shown in Section 2.2, the filamentary turns are replaced by coils, as shown in Fig.4. Neglecting gap among turns, then the number of turns in per unit area of cross section of the coil is $\dfrac{N}{hw}$. The formula of electrical field intensity can be obtained by integrating $E_{\varphi 2}$ over the cross-section of the coil per unit area. It is shown below:

$$E_{\varphi} = -\frac{j\omega\mu_1 I_{\varphi}}{l}\frac{N}{hw}$$

$$\times \int_{a_1}^{a_2}\int_{-\frac{w}{2}}^{\frac{w}{2}}\left[\frac{\mu_{2r}I_1(mr)}{mI_0(mb)} + 2\sum_{k=1}^{\infty}aK_1(\beta_k a)\right.$$

$$\left.\times\frac{I_1(\Gamma_k r)I_1(\beta_k b)}{I_1(\Gamma_k b)}\Phi(\beta_k)\cos\beta_k(z-\tau)\right]d\tau da \qquad (16)$$

The internal integrals are readily evaluated to give the formula:

$$E_{\varphi} = E_{\varphi 0} + E_{\varphi k} \qquad (17)$$

where

$$E_{\varphi 0} = -\frac{j\omega\mu_1 NI_{\varphi}}{l}\frac{\mu_{2r}I_1(mr)}{mI_0(mb)} \qquad (18)$$

$$E_{\varphi k} = -\frac{j\omega\mu_1 NI_{\varphi}}{l}\left[\frac{2}{hw}\sum_{k=1}^{\infty}P_1(\beta_k a_2,\beta_k a_1)R_1(\beta_k w)\right. \qquad (19)$$

$$\left.\times\frac{I_1(\Gamma_k r)I_1(\beta_k b)}{I_1(\Gamma_k b)}\Phi(\beta_k)\cos(\beta_k z)\right]$$

where

$$P_1(\beta x,\beta y) = \frac{1}{\beta^2}\left[p_1(\beta x) - p_1(\beta y)\right]$$

$$p_1(\alpha) = \frac{\pi\alpha}{2}\left[K_1(\alpha)L_0(\alpha) + L_1(\alpha)K_0(\alpha)\right]$$

$L_0(x)$, $L_1(x)$ — the modified Struve functions

$$R_1(\beta x) = \frac{2}{\beta}\sin\frac{\beta x}{2}$$

In Eqn.17 E_{φ} is decomposed into $E_{\varphi 0}$ and $E_{\varphi k}$. It is noted that $E_{\varphi 0}$ is unrelated to z, i.e. it is a constant value along the axial direction. But $E_{\varphi k}$ is a function of z.

3 Magnetic field intensity in the core

On the basis of Maxwell's equation $H = -\frac{1}{j\omega\mu}\nabla\times E$ and Eqn.17, we have

$$H_r = \frac{2NI_{\varphi}}{l\mu_{2r}hw}\sum_{k=1}^{\infty}P_1(\beta_k a_2,\beta_k a_1)R_1(\beta_k w)$$

$$\times\frac{I_1(\Gamma_k r)I_1(\beta_k b)}{I_1(\Gamma_k b)}\Phi(\beta_k)\beta_k\sin(\beta_k z) \qquad (20)$$

$$H_z = H_{z0} + H_{zk} \qquad (21)$$

where

$$H_{z0} = \frac{NI_{\phi}}{l}\frac{I_0(mr)}{I_0(mb)} \qquad (22)$$

$$H_{zk} = \frac{2NI_{\varphi}}{l\mu_{2r}hw}\sum_{k=1}^{\infty}P_1(\beta_k a_2,\beta_k a_1)R_1(\beta_k w)$$

$$\times\frac{\Gamma_k I_0(\Gamma_k r)I_1(\beta_k b)}{I_1(\Gamma_k b)}\Phi(\beta_k)\beta_k\cos(\beta_k z) \qquad (23)$$

H_r is the component of the magnetic field intensity in the radius direction and H_z is the component of the magnetic field intensity in the axial direction. Similar to E_{φ}, H_z is also decomposed into H_{z0} and H_{zk}. H_{z0} is unrelated to z, indicating it is a constant value along the axial direction. But H_{zk} is a function of z.

4 Eddy-current power losses in the core

Formula about electrical field intensity E and average power P in isotropic linear medium is written as follows:

$$P = \int_V \sigma|E|^2 dV \qquad (24)$$

Substituting Eqn.17 into Eqn.24, eddy-current power losses in the toroidal core can be obtained as

$$P_J = 2\pi\int_{-\frac{l}{2}}^{\frac{l}{2}}\int_0^b \sigma|E_{\varphi}|^2 r\,dr\,dz$$

$$= \frac{2\pi(\omega\mu_1 I_{\varphi}N)^2\sigma}{l}\left|\frac{\mu_{2r}}{mI_0(mb)}\right|\frac{b}{m^2-\overline{m}^2} \qquad (25)$$

$$\times\left[mI_1(\overline{m}b)I_0(mb) - \overline{m}I_1(mb)I_0(\overline{m}b)\right]$$

$$+\frac{2}{h^2\omega^2}\sum_{k=1}^{\infty}\left|P_1(\beta_k a_2,\beta_k a_1)R_1(\beta_k\omega)\Phi(\beta_k)\frac{I_1(\beta_k b)}{I_1(\tau_k b)}\right|$$

$$\times\frac{b}{\tau_k^2-\overline{\tau}_k^2}\left[\tau_k I_1(\overline{\tau}_k b)I_0(\tau_k b) - \overline{\tau}_k I_1(\tau_k b)I_0(\overline{\tau}_k b)\right]$$

5 Verification

The real part of impedance give the eddy-current losses in the core in the form of a series resistance [11]. Therefore, in order to validate accuracy of Eqn.25 another formula of eddy-current power losses is given herein

$$P_Z = I_{\varphi}^2\,\text{Re}(Z_{mm}) \qquad (26)$$

where Z_{mm} is self-impedance which is given in Ref.[9]:

$$Z_{mm} = \frac{j\omega\mu_1\pi b^2}{l}N^2\left(\frac{2\mu_{2r}I_1(mb)}{mbI_0(mb)} - 1\right)$$

$$+\frac{j\omega\mu_1\pi}{l}\frac{4N^2}{h^2w^2}\sum_{k=1}^{\infty}[P_1(\beta_k a_2,\beta_k a_1)]^2$$

$$\times Q_1(\beta_k w)\frac{I_1(\beta_k b)}{K_1(\beta_k b)}F(\beta_k)$$

where

$$F(\beta) = \frac{f(\beta) + \frac{\mu_1}{\mu_2}f(\Gamma)}{g(\beta) + \frac{\mu_1}{\mu_2}f(\Gamma)}$$

$$Q_1(\beta_k w) = \frac{2}{\beta_k^2}\left(1 - \cos\beta_k w\right)$$

Where function $f(x)$ and $g(x)$ are defined by Eqn.4 and Eqn.5.

Tab.1 Dimensions and properties of core and coil

Core radius	$b = 10.8\text{mm}$
Number of turns	$N = 25$
Coil inside radius	$a_1 = 15\text{mm}$
Coil outside radius	$a_2 = 25\text{mm}$
Coil width	$w = 10\text{mm}$
Magnetic path length	$l = 250\text{mm}$
Relative permeability	$\mu_{2r} = 75$
Core conductivity	$\sigma = 100\text{S} \cdot \text{m}^{-1}$

For the comparison, calculations were carried out on a Micrometals T400-26 10cm O.D. powdered core with a distributed gap. Full details of the core and coil are given in Tab.1, which are the same as those used in Ref.[10].

In the following, we use Eqn.25 and Eqn.26 to calculate eddy-current power losses at different frequency, respectively. The results are shown in Tab.2. It is found that the calculated results agree well with each other, validating the accuracy of Eqn.25. Thus the accuracy of Eqn.17, 20 and 21 have also been verified.

Tab.2 Comparison of results from Eqn.25 and Eqn. 26

f (Hz)	P_J (W)	P_Z (W)
10^3	4.684×10^{-4}	4.675×10^{-4}
10^4	4.683×10^{-2}	4.674×10^{-2}
10^5	4.621	4.612
10^6	204.113	203.743

6 Results and discussion

6.1 Electromagnetic field distributions

For magnetic component in section 5, electrical field intensity and magnetic field intensity are calculated for various position of the core
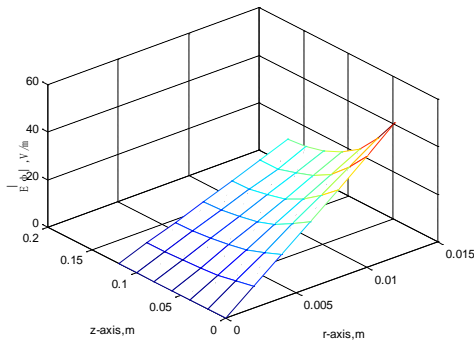

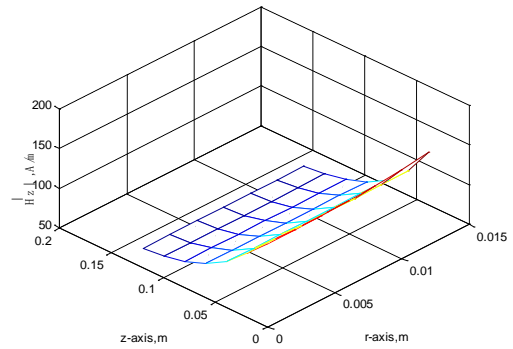**Fig.5 Amplitude of E_φ at $f = 100\text{KHz}$**

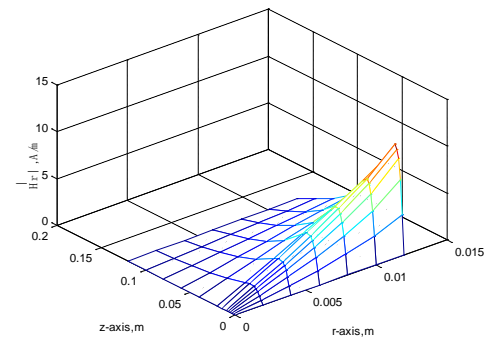**Fig.6 Amplitude of H_z at $f = 100\text{KHz}$**

Fig.7 Amplitude of H_r at $f = 100\text{KHz}$

at $f = 100\text{KHz}$. The calculated results are shown in Figs.5-7.

From the curve shown in Fig.5 and Fig.6, it is found that with the increasing of z, both $|E_\varphi|$ and $|H_z|$ decrease pronouncedly. This result is due to the fact that there are relatively large leakage fluxes in the core. With the increasing of r, $|E_\varphi|$ and $|H_z|$ both increase too. This result is due to skin effect. H_r is normal component of magnetic field intensity. Magnetic fluxes which arise from H_r are leakage fluxes. Fig.6 and Fig.7 indicate that $|H_r|$ is much smaller than $|H_z|$. When z is zero, $|H_r|$ is zero too. Then it has a substantial increase and reaches the maximal value at about $z = 15\text{mm}$. Thereafter it has a substantial decrease. At $z = 120\text{mm}$ its value approximately decrease to zero. It has been shown that normal leakage flux effects are concentrated mainly

around the windings.

6.2 Leakage flux analysis

On the basis of Eqn.21, formula of magnetic fluxes in homogeneous linear isotropic medium can be obtained as follows

$$\Phi = \int \mu_2 H_z \mathrm{d}s = \int_0^b \mu_2 H_z 2\pi r \mathrm{d}r$$

$$= \frac{2\pi N I_\varphi \mu_2 b}{lm} \frac{I_1(mb)}{I_0(mb)} + \frac{4\pi N I_\phi \mu_1}{lhw} \sum_{k=1}^\infty P_1(\beta_k a_2, \beta_k a_1) \quad (27)$$

$$\times R_1(\beta_k w) b I_1(\beta_k b) \Phi(\beta_k) \beta_k \cos(\beta_k z)$$

6.2.1 Effect of frequency on leakage fluxes

For magnetic component shown in Fig.1, except magnetic permeability μ_{2r}, the rest parameters are the same as those given in Tab.1. Magnetic fluxes are calculated at $\mu_{2r} = 10^3$ for different frequency. The calculated results are shown in Tab.3.

Φ_0 is defined as magnetic fluxes at $z = 0$ and Φ_1 is magnetic fluxes at $z = 120\mathrm{mm}$. Thus leakage fluxes at $z = 120\mathrm{mm}$ can be defined as $\Delta\Phi = \Phi_0 - \Phi_1$. The proportion of leakage fluxes can be defined as $\Delta\Phi/\Phi_0$. The calculated results of the leakage fluxes and the proportion of leakage fluxes are shown in Tab.4.

Tab.3 Magnetic fluxes for different frequency at $\mu_{2r} = 10^3$

$f(Hz)$ / $\Phi(Web)$ / $z(mm)$	10^3	10^4	10^5	10^6	10^7
0	4.83×10^{-5}	4.79×10^{-5}	2.99×10^{-5}	1.11×10^{-5}	4.81×10^{-6}
40	4.64×10^{-5}	4.59×10^{-5}	2.83×10^{-5}	9.51×10^{-6}	3.23×10^{-6}
80	4.53×10^{-5}	4.48×10^{-5}	2.74×10^{-5}	8.73×10^{-6}	2.53×10^{-6}
120	4.50×10^{-5}	4.44×10^{-5}	2.71×10^{-5}	8.48×10^{-6}	2.31×10^{-6}

Tab.4 leakage fluxes and the proportion of leakage fluxes at $\mu_{2r} = 10^3$

$f(Hz)$	10^3	10^4	10^5	10^6	10^7
$\Delta\Phi$	3.3×10^{-6}	3.5×10^{-6}	2.8×10^{-6}	2.62×10^{-6}	2.50×10^{-6}
$\Delta\Phi/\Phi_0$	6.8%	7.3%	9.6%	23.6%	52.0%

Tab.3 and Tab.4 indicate that the proportion of

leakage fluxes increase with the increasing of frequency, while magnetic fluxes decrease. At higher frequencies this phenomenon becomes more obvious. For example, as $f = 10^7 \mathrm{Hz}$ the value of magnetic fluxes is only 10% comparing to the frequency is $f = 10^3 \mathrm{Hz}$, the proportion of leakage fluxes reaches 52%. The deterioration in performance, accurately predicted by the formula, explain why the manufacturers deem the core unsuitable for operation above 50KHz

6.2.2 Effect of magnetic permeability on leakage fluxes

For magnetic component shown in Fig.1, except magnetic permeability μ_{2r}, the rest parameters are the same as those given in Tab.1. Magnetic permeability is varied. Magnetic fluxes are calculated at $f = 1\mathrm{MHz}$ for different magnetic permeability. The calculated results are shown in Tab.5.

Definition of Φ_0、Φ_1、$\Delta\Phi$、$\Delta\Phi/\Phi_0$ is same as above. The calculated results of leakage fluxes and the proportion of leakage fluxes are shown in Tab.6.

Tab.5 Magnetic fluxes for different magnetic permeability at $f = 1\mathrm{MHz}$

μ_{2r} \ $\Phi(Web)$ \ $z(mm)$	0	40	80	120
10^2	4.67×10^{-6}	3.03×10^{-6}	2.30×10^{-6}	2.07×10^{-6}
10^3	1.11×10^{-5}	9.51×10^{-6}	8.73×10^{-6}	8.48×10^{-6}
10^4	3.17×10^{-5}	3.02×10^{-5}	2.95×10^{-5}	2.92×10^{-5}
10^5	9.73×10^{-5}	9.58×10^{-5}	9.51×10^{-5}	9.48×10^{-5}

Tab.6 leakage fluxes and the proportion of leakage fluxes at $f = 1\mathrm{MHz}$

μ_{2r}	10^2	10^3	10^4	10^5
$\Delta\Phi$	2.60×10^{-6}	2.62×10^{-6}	2.50×10^{-6}	2.50×10^{-6}
$\Delta\Phi/\Phi_0$	55.6%	23.6%	7.9%	2.5%

Tab.5 and Tab.6 indicate when magnetic permeability is small magnetic fluxes are small, the proportion of leakage fluxes are large. For

example, at $\mu_{2r} = 10^2$ the proportion of leakage fluxes reaches 55.6%, more than half of the magnetic fluxes. With the increasing of magnetic permeability magnetic fluxes increase, while the proportion of leakage fluxes decrease. At $\mu_{2r} = 10^5$ leakage fluxes are small, the proportion of leakage fluxes reduce to 2.5%, indicating when magnetic permeability of the core is very large, leakage fluxes are very small and can be neglected, as referred to before. On this occasion, electrical field intensity and magnetic field intensity are calculated at $r = 10\text{mm}$. The calculated results are shown in Tab.7 and Tab.8.

Tab.7 Amplitude of electrical field intensity at $f = 1\text{MHz}$, $\mu_{2r} = 10^5$, $r = 10\text{mm}$

z(mm)	$|E_{\varphi0}|$(V/m)	$|E_{\varphi k}|$(V/m)	$|E_\varphi|$(A/m)
0	60.4	1.49	61.4
40	60.4	0.22	60.5
80	60.4	0.45	60.3
120	60.4	0.69	60.0

Tab.8 Amplitude of magnetic field intensity at $f = 1\text{MHz}$, $\mu_{2r} = 10^5$, $r = 10\text{mm}$

z(mm)	$|H_{z0}|$(A/m)	$|H_{zk}|$(A/m)	$|H_z|$(A/m)	$|H_r|$(A/m)
0	0.68	0.017	0.69	0
40	0.68	0.003	0.68	3.1×10^{-5}
80	0.68	0.005	0.68	1.4×10^{-5}
120	0.68	0.008	0.68	1.5×10^{-6}

From Tab.7 and Tab.8 it is found that

$$|E_\varphi| \approx |E_{\varphi0}|$$
$$|E_{\varphi k}| << |E_{\varphi0}|$$
$$|H_z| \approx |H_{z0}|$$
$$|H_{zk}| \approx 0$$
$$|H_r| \approx 0$$

It has been shown that in this case $E_{\varphi k}$, H_{zk} and H_r can be neglected. Thus magnetic field only has axial direction component. Both E_φ and H_z are constant value along the axial direction.

6.2.3 Effect of windings distribution on leakage fluxes

For magnetic component shown in Fig.1, parameters of the core are the same as those given in Tab.1, while parameters of the coil are varied. Here Magnetic fluxes are calculated only for a particular case when the coil is wound densely and uniformly on the surface of the core. Parameters of the coil are given as follows: $NI_\phi = 25A$, $w = l = 250\text{mm}$, $a_1 \approx b = 10.8\text{mm}$, $h = 1\text{mm}$, thus $a_2 = 11.8\text{mm}$. Magnetic fluxes are calculated at $f = 1\text{MHz}$. The calculated results are shown in Tab.9.

Tab.9 Magnetic fluxes when the coil is wound densely and uniformly on the surface of the core at $f = 1\text{MHz}$, $\mu_{2r} = 75$

z(mm)	0	40	80	120
Φ(Web)	4.55×10^{-6}	4.55×10^{-6}	4.55×10^{-6}	4.55×10^{-6}

From Tab.9 it is found that when the coil is wound densely and uniformly on the surface of the core, even if magnetic permeability is small（in this numerical example $\mu_{2r} = 75$）and frequency is high, leakage fluxes are very small, therefore they can be neglected. On this occasion, electrical field intensity and magnetic field intensity are calculated at $r = 10\text{mm}$. Calculated results are shown in Tab.10 and Tab.11.

Tab.10 Amplitude of electrical field intensity when the coil is wound densely and uniformly on the surface of the core at $f = 1\text{MHz}$, $\mu_{2r} = 75$, $r = 10\text{mm}$

z(mm)	$|E_{\varphi0}|$(V/m)	$|E_{\varphi k}|$(V/m)	$|E_\varphi|$(A/m)
0	200.6	4.4×10^{-5}	200.6
40	200.6	3.5×10^{-5}	200.6
80	200.6	2.4×10^{-5}	200.6
120	200.6	1.2×10^{-6}	200.6

Tab.11 Amplitude of magnetic field intensity when the coil is wound densely and uniformly on the surface of the core at $f = 1\text{MHz}$, $\mu_{2r} = 75$, $r = 10\text{mm}$

z(mm)	$|H_{z0}|$(A/m)	$|H_{zk}|$(A/m)	$|H_z|$(A/m)	$|H_r|$(A/m)
0	91.1	2.0×10^{-5}	91.1	0
40	91.1	1.6×10^{-5}	91.1	9.1×10^{-7}
80	91.1	1.0×10^{-5}	91.1	2.3×10^{-6}
120	91.1	5.1×10^{-6}	91.1	1.5×10^{-6}

From Tab.10 and 11 it is found that

$$\left|E_\varphi\right| \approx \left|E_{\varphi 0}\right|$$
$$\left|E_{\varphi k}\right| \approx 0$$
$$\left|H_z\right| \approx \left|H_{z0}\right|$$
$$\left|H_{zk}\right| \approx 0$$
$$\left|H_r\right| \approx 0$$

Similar to the case when magnetic permeability is very large, $E_{\varphi k}$, H_{zk} and H_r can also be neglected. Thus magnetic field only has axial direction component. Both E_φ and H_z are constant value along the axial direction.

7 Conclusion

In this paper, toroidal core with circular cross section is considered. An Analytic method is used for electromagnetic field distributions and eddy-current power losses for toroidal core, in which the field variables are expressed as a single series in terms of Bessel functions and trigonometric functions. It is not only applicable to the case when coil is wound partially on the surface of the core, with taking into account leakage fluxes, but also applicable to the case when magnetic permeability of the core is very large or the coil is wound densely and uniformly on the surface of the core,with neglecting leakage fluxes.

Results presented in the study show a classical separation of formulas of electrical field intensity and magnetic field intensity into two components respectively, one component ($E_{\varphi 0}, H_{z0}$) is constant along the axial direction, whereas the other component ($E_{\varphi k}, H_{zk}$) is variable. The proportion of the variable component decreases with increasing of magnetic permeability. When magnetic permeability of the core is very large (in the numerical example of this paper $\mu_{2r} > 10^5$) or the coil is wound densely and uniformly on the surface of the core, the variable component is so small that it can be neglected.

References

[1] Belove C. Handbook of modern electronics and electrical engineering[M]. New York ： Wiley,1986,159-160,248.

[2] Wang Zhao'an, Zhang Mingxun. Application handbook of Power electronic devices [M]. Beijing： China Machine Press, 2002,702-745.

[3] Han Shuai, Zhang Li, Tan Xingguo. Material selection based on loss characterization for high-power high-frequency transformer cores [J]. High Voltage Engineering, 2012,38(6):1486-1491.

[4] Ying Baiqing . FEM solutions of eddy-current power loss in toroidal cores with arhitray cross section [J]. Microelectronics & Computer, 2002,(4): 51-53.

[5] K V Namjoshi, J Douglas lavers, P P Biringer. Eddy current power loss in toroidal cores with rectangular cross section [J]. IEEE Transactions on Magnetics, 1988, 34(3): 636-641.

[6] Ma Xikui, Zhao Yanzhen, Dai Dong . Analytical solution of eddy-current power loss in toroidal cores with rectangular cross section for high-frequency electronic circuits [J]. Proceeding of the CSEE, 2005, 25(6): 124-128.

[7] Saotome H, Sakaki Y. Iron loss analysis of Mn-Zn ferrite cores[J]. IEEE Transactions on Magnetics,1997, 33(1): 728-734.

[8] Daming Zhang, Chek Fok Foo. Theoretical analysis of the electrical and magnetic field distributions in a toroidal core with circular cross section[J]. IEEE Transactions on Magnetics, 1999, 35(3): 1924-1931.

[9] Wilcox D J, Conlon M , Hurley W G. Calculation of self and mutual impedances for coils on ferromagnetic cores[J]. IEE Proceedings, 1988, 135(7): 470-476.

[10] William G Hurley , David J Wilcox. Calculation of leakage inductance in transformer windings[J]. IEEE Transactions on Power Electronics, 1994, 9(1): 121-126.

[11] W M Gerard Hurley, David J Wilcox. Calculation of short circuit impedance and leakage impedance in transformer windings [A].Power Electronics Specialists Conference, PESC' 91 Record 22nd Annual IEEE[C]. 1991.651-658.